



## Increases in reactive oxygen species enhance vascular endothelial cell migration through a mechanism dependent on the transient receptor potential melastatin 4 ion channel

Daniela Sarmiento<sup>a,1</sup>, Ignacio Montorfano<sup>a,1</sup>, Oscar Cerda<sup>d</sup>, Mónica Cáceres<sup>f</sup>, Alvaro Becerra<sup>a</sup>, Claudio Cabello-Verrugio<sup>a</sup>, Alvaro A. Elorza<sup>a,c</sup>, Claudia Riedel<sup>a,c</sup>, Pablo Tapia<sup>g</sup>, Luis A. Velásquez<sup>b,h</sup>, Diego Varela<sup>e</sup>, Felipe Simon<sup>a,c,\*</sup>

<sup>a</sup> Departamento de Ciencias Biológicas, Facultad de Ciencias Biológicas, Universidad Andres Bello, Santiago, Chile

<sup>b</sup> Center for Integrative Medicine and Innovative Science (CIMIS), Facultad de Medicina, Universidad Andres Bello, Santiago, Chile

<sup>c</sup> Millennium Institute on Immunology and Immunotherapy, Santiago, Chile

<sup>d</sup> Programa de Biología Celular y Molecular, Instituto de Ciencias Biomédicas, Facultad de Medicina, Universidad de Chile, Santiago, Chile

<sup>e</sup> Programa de Fisiopatología, Centro de Estudios Moleculares de la Célula and Instituto de Ciencias Biomédicas, Facultad de Medicina, Universidad de Chile, Santiago, Chile

<sup>f</sup> Facultad de Medicina, Pontificia Universidad Católica de Chile, Santiago, Chile

<sup>g</sup> Departamento de Medicina Intensiva, Facultad de Medicina, Pontificia Universidad Católica de Chile, Santiago, Chile

<sup>h</sup> Centro para el Desarrollo de la Nanociencia y Nanotecnología, Universidad de Santiago de Chile, Santiago, Chile

### ARTICLE INFO

#### Article history:

Accepted 3 February 2014

Available online 9 February 2014

### ABSTRACT

A hallmark of severe inflammation is reactive oxygen species (ROS) overproduction induced by increased inflammatory mediators secretion. During systemic inflammation, inflammation mediators circulating in the bloodstream interact with endothelial cells (ECs) raising intracellular oxidative stress at the endothelial monolayer. Oxidative stress mediates several pathological functions, including an exacerbated EC migration. Because cell migration critically depends on calcium channel-mediated  $\text{Ca}^{2+}$  influx, the molecular identification of the calcium channel involved in oxidative stress-modulated EC migration has been the subject of intense investigation.

The transient receptor potential melastatin 4 (TRPM4) protein is a ROS-modulated non-selective cationic channel that performs several cell functions, including regulating intracellular  $\text{Ca}^{2+}$  overload and  $\text{Ca}^{2+}$  oscillation. This channel is expressed in multiple tissues, including ECs, and contributes to the migration of certain immune cells. However, whether the TRPM4 ion channel participates in oxidative stress-mediated EC migration is not known. Herein, we investigate whether oxidative stress initiates or enhances EC migration and study the role played by the ROS-modulated TRPM4 ion channel in oxidative stress-mediated EC migration.

We demonstrate that oxidative stress enhances, but does not initiate, EC migration in a dose-dependent manner. Notably, we demonstrate that the TRPM4 ion channel is critical in promoting  $\text{H}_2\text{O}_2$ -enhanced EC migration. These results show that TRPM4 is a novel pharmacological target for the possible treatment of severe inflammation and other oxidative stress-mediated inflammatory diseases.

© 2014 Elsevier Inc. All rights reserved.

### Introduction

It is well-accepted that inflammatory diseases are inexorably accompanied by an increased reactive oxygen species (ROS) concentration through increases in ROS production and a decrease in the cellular reducing capacity (Closa and Folch-Puy, 2004; Droge, 2002). ROS comprises a group of oxidative molecules that include the

superoxide radical ( $\text{O}_2^-$ ), hydrogen peroxide ( $\text{H}_2\text{O}_2$ ), and the hydroxyl radical ( $\cdot\text{OH}$ ) (Droge, 2002). While low ROS concentrations are necessary for normal cellular processes, high ROS levels have deleterious effects on cells (Bryan et al., 2012; Cabello-Verrugio et al., 2011; Droge, 2002; Echeverria et al., 2013; Morales et al., 2012; Nagata, 2005; Nunez-Villena et al., 2011). ROS-induced damage is principally due to protein modification, which alters their function and promotes abnormal cell processes (Droge, 2002; Griendling et al., 2000).

In contrast to mild inflammation, during acute and chronic severe inflammation, the immune system produces an uncontrolled inflammatory response involving oversecreted inflammation mediators, including pro-inflammatory cytokines and cell-derived proteins (Closa and Folch-Puy, 2004; Nagata, 2005). The cell response generated by the

\* Corresponding author at: Departamento de Ciencias Biológicas, Facultad de Ciencias Biológicas and Facultad de Medicina, Universidad Andres Bello. Av. Republica 252, 8370134 Santiago, Chile. Fax: +56 2 2698 0414.

E-mail address: [fsimon@unab.cl](mailto:fsimon@unab.cl) (F. Simon).

<sup>1</sup> These authors contributed equally to this work.

mediators of inflammation is characterized by ROS overproduction, which increases cellular oxidative stress (Cai and Harrison, 2000; Closa and Folch-Puy, 2004; Nagata, 2005).

For systemic inflammation, high levels of inflammation mediators are released in the bloodstream and can directly interact with endothelial cells (ECs) in the inner wall of blood vessels (Closa and Folch-Puy, 2004; Muller and Griesmacher, 2000), which increases ROS production and, thus, raises intracellular oxidative stress in ECs. Therefore, ROS interact with the endothelial monolayer and raise the intracellular level of oxidative stress in ECs.

Oxidative stress mediates several physiological and pathological functions. ROS is involved in cell migration for several cell types. ROS has been shown to regulate migration for smooth muscle cells (Lo et al., 2005; Lu et al., 2013; Wang et al., 2004a, 2004b), immune cells (Cook-Mills, 2002; Van der Goes et al., 2001), astrocytes (Lin et al., 2012), and lung cancer cells (Luanpitpong et al., 2010), among others.

Specifically for ECs, augmented oxidative stress stimulates EC migration. Vascular endothelial growth factor (VEGF)-induced human EC migration is stimulated via NAD(P)H oxidase (NOX)-derived ROS production in a Rac1-dependent mechanism (Coso et al., 2012; Ikeda et al., 2005; Kaplan et al., 2011; Stone and Collins, 2002; Ushio-Fukai, 2006; Yamaoka-Tojo et al., 2004). Furthermore, a role for ROS generated by NOX-2 and NOX-4 in EC migration has been demonstrated (Pendyala et al., 2009). In addition, VEGF-induced EC migration was suppressed by adding the antioxidant vitamin E to mitochondria and overexpressing mitochondrial catalase (Wang et al., 2011). Similar results were generated through mitochondrial DNA depletion (Wang et al., 2011). These findings suggest a role for ROS in promoting EC migration.

Cell migration depends on  $\text{Ca}^{2+}$  influx-induced intracellular calcium changes to produce  $[\text{Ca}^{2+}]$  gradients (Goumans et al., 2008; Potenta et al., 2008). Several studies have shown that changes in intracellular calcium concentrations are a decisive step in EC migration (Kimura et al., 2001; Tran et al., 1999). Inhibiting  $\text{Ca}^{2+}$  influx through channel blockers markedly abolishes EC migration (Wu et al., 1997; Yoshikawa et al., 1999). Nonetheless, the molecular identity of the ion channel involved in controlling  $\text{Ca}^{2+}$  influx during oxidative stress-mediated EC migration remains unknown.

The transient receptor potential melastatin 4 (TRPM4) is a  $\text{Ca}^{2+}$ -activated non-selective ion channel permeable to monovalent cations, such as  $\text{Na}^+$  and  $\text{K}^+$ , but is virtually impermeable to divalent ions, such as  $\text{Ca}^{2+}$  and  $\text{Mg}^{2+}$  (Launay et al., 2002; Nilius et al., 2003). TRPM4 performs several cell functions, including regulating intracellular  $\text{Ca}^{2+}$  overload and  $\text{Ca}^{2+}$  oscillation control (Launay et al., 2002, 2004; Nilius et al., 2003), and it is expressed in multiple tissues, including arterial and vein-derived ECs (Becerra et al., 2011; Fantozzi et al., 2003). We previously reported that TRPM4 activity is also modulated by oxidative stress (Becerra et al., 2011; Simon et al., 2010, 2013). Exposing TRPM4 to  $\text{H}_2\text{O}_2$  abolished channel desensitization, which yielded sustained TRPM4 activity without changes in the  $[\text{Ca}^{2+}]_i$  dependence (Simon et al., 2010). In addition, TRPM4 is involved in immune cell migration as bone marrow-derived mast cells (BMMCs) (Shimizu et al., 2009), T lymphocyte migration (Weber et al., 2010), and chemokine-dependent dendritic cell migration (Barbet et al., 2008).

Therefore, TRPM4 is a potential EC migration regulator during oxidative stress conditions. However, whether the TRPM4 ion channel participates in oxidative stress-mediated EC migration is unknown.

Herein, we investigated whether oxidative stress initiates or enhances EC migration and evaluated the role of the ROS-modulated TRPM4 ion channel in oxidative stress-mediated EC migration.

We demonstrate that  $\text{H}_2\text{O}_2$  enhances, but not initiates, EC migration in a dose-dependent manner. Noteworthy, we demonstrate that the TRPM4 ion channel is critical for promoting  $\text{H}_2\text{O}_2$ -enhanced EC migration.

These findings contribute to determining the molecular mechanism underlying oxidative stress-mediated EC migration. These results show that the TRPM4 ion channel is a novel pharmacological target against

severe inflammation and other oxidative stress-mediated inflammatory diseases.

## Materials and methods

Details of all procedures are provided in Online Supplementary Material.

### Cell culture

Human umbilical vein endothelial cells (HUVEC) were isolated by collagenase (0.25 mg/mL) digestion from freshly obtained umbilical cord veins from normal pregnancies, after patient's informed consent. The investigation conforms with the principles outlined in the Declaration of Helsinki. The Commission of Bioethics and Biosafety of Universidad Andres Bello approved all experimental protocols. Cells were grown in gelatin-coated dishes at 37 °C in a 5%:95%  $\text{CO}_2$ :air atmosphere in medium 199 (Sigma, MO), containing 100  $\mu\text{g}/\text{mL}$  endothelial cell growth supplement (ECGS) (Sigma), 100  $\mu\text{g}/\text{mL}$  heparin, 5 mmol/L D-glucose, 3.2 mmol/L L-glutamine, 10% fetal bovine serum (FBS) (GIBCO, NY), and 50 U/mL penicillin–streptomycin (Sigma-Aldrich, St Louis, USA).

### Cell adhesion assay

For cell adhesion experiments, cells were harvested using trypsin, washed and then incubated in the absence or presence of different  $\text{H}_2\text{O}_2$  concentrations for 15 min in the presence of 1% FBS. Then, 10,000 cells per well were seeded over gelatin-coated 96-well plates (Falcon, Becton Dickinson, CA, USA) at 37 °C for 20 min in M199 plus 1% FBS. Cell adhesion was stopped by pouring off the medium. After washing, cells were fixed with 10% ethanol for 5 min and stained with 0.2% crystal violet for 5 min. After removing excess of dye, cells were solubilized in 0.1 M  $\text{NaH}_2\text{PO}_4$  in 50% ethanol for 15 min at room temperature (RT). Absorbance at 570 nm was analyzed on a microplate reader. All assays were performed at least in triplicates in three separate sets of experiments.

### Cell-spreading assay

For cell-spreading experiments, cells were harvested using trypsin, washed and then incubated in the absence or presence of different  $\text{H}_2\text{O}_2$  concentrations for 15 min in the presence of 1% FBS. Then, 10,000 cells per well were seeded over gelatin-coated 24-well plates (Falcon) at 37 °C for 40 min in M199 plus 1% FBS. After washing, cells were fixed with 10% ethanol for 5 min and stained with 0.2% crystal violet for 5 min. After removing excess of dye, spread and non-spread cells were identified through microscopic visualization and counted. Images were captured through a digital microscope system. The ratio spread/total cells was calculated for each set of experimental conditions after counting four fields per set of conditions. All assays were performed at least in triplicates in three separate sets of experiments.

### Cell migration measurement by Transwell assay

ECs migration was assayed using Transwell chambers (Costar, Cambridge, MA, USA) with 8.0- $\mu\text{m}$ -pore polycarbonate filters. Cells were harvested using trypsin, washed and then seeded in the absence or presence of different  $\text{H}_2\text{O}_2$  concentrations for 24 h in medium containing 1% FBS on the upper compartment of the chamber. To stimulate cell migration, 10% FBS was added to the lower compartment of the chamber. Thus, migration was allowed to occur for 24 h. After washing, non-invading cells were removed from the upper surface of the membrane with a cotton swab. The invading cells were fixed with 10% ethanol for 5 min and stained with 0.2% crystal violet for 5 min. Images were captured through a digital microscope system. Cell migration was

evaluated by counting four fields per chamber in every condition. All assays were performed at least in triplicates in three separate sets of experiments.

#### *Cell migration measurement by wound-closure assay*

ECs were harvested using trypsin, washed and then seeded until reached a monolayer. Then, cell culture were scratched with a 10  $\mu$ L sterile tip and washed to remove detached cells and debris. Cells were then incubated in medium containing 1% FBS and different  $H_2O_2$  concentrations. After 8 h cells were fixed with methanol for 2 min. Images of each wound were captured through a digital microscope system (Motic microscope AE31 with moticam 2300, Motic Instruments Inc., Hong Kong, China). The ratio of wound closure percentage was determined using a software analysis system (Motic Images Plus 2.0, Motic Instruments Inc.). In brief, cell margins were outlined in each image, and the uncovered area of each wound was compared between vehicle-treated cells and vehicle-treated cells. For the quantification of the migrated distance in the wound-closure assay, the lineal migrated distance of several cells was measured at 8 h. All assays were performed at least in triplicates in three separate sets of experiments.

#### *Small interfering RNA against TRPM4 and transfections*

SiGENOME SMARTpool siRNA against TRPM4 (four separated siRNAs per TRPM4 transcript) were purchased from Dharmacon (Dharmacon, Lafayette, CO). Non-targeting siRNA (siRNA-CTRL) was used as a control. In brief, HUVEC were plated overnight in 24-well plate and then transfected with 5 nM siRNA of siRNA-CTRL or siRNA-TRPM4 using DharmaFECT 4 transfection reagent (Dharmacon) used according to the manufacturer's protocols in serum-free medium in Opti MEM (Gibco) for 6 h.

#### *Quantitative PCR and Western blotting for TRPM4*

Cells transfected with siRNA-CTRL or siRNA-TRPM4 were subjected to qPCR and Western blotting for TRPM4. QPCR: Total RNA was extracted with Trizol according to the manufacturer's protocol (Invitrogen, Carlsbad, CA). DNase I-treated RNA was used for reverse transcription using the Super Script II Kit (Invitrogen, Carlsbad, CA). Equal amounts of RNA were used as templates in each reaction. QPCR was performed using SYBR Green PCR Master Mix (AB Applied Biosystems, Foster City, CA). Data are presented as relative mRNA levels of the gene of interest normalized to relative levels of 28S mRNA. Western blotting: Whole cell extracts were subjected to 12% SDS-PAGE. Resolved proteins were transferred to a nitrocellulose membrane, blocked, and then incubated ON with the anti-TRPM4 antibody (Origene, Rockville, MD). Tubulin was used as a loading control (Sigma). TRPM4 protein content was determined by densitometric scanning of immunoreactive bands and intensity values were obtained by densitometry of individual bands compared with tubulin and normalized against siRNA-CTRL. Details of procedures, primers sequences, PCR protocols, and further details are provided in the online supplement.

#### *Cell depolarization measurements*

Cells were grown in medium containing 1% FBS and loaded with 150 nM of the cell membrane depolarization indicator bis-(1,3-dibutylbarbituric acid) trimethine oxonol (DiBAC4(3)) for 30 min at 25 °C and fluorescence was measured at 488 nm. Briefly, in the resting state, DiBAC4(3) is excluded from the cell. Upon plasma membrane depolarization, DiBAC4(3) enters into the cell and can be detected with flow cytometry analysis by the increase in fluorescence. Experiments were performed using a FACSCanto flow cytometry system and analysis was performed using FACSDiva software (BD Biosciences, CA, USA). A minimum of 15,000 viable cells/sample was analyzed.

#### *Reagents*

Hydrogen peroxide, buffers and salts were purchased from Merck Biosciences (Darmstadt). PMA, NAC, DPI and APO were purchased from Sigma-Aldrich (St. Louis, MO).

#### *Data analysis*

All results are presented as mean  $\pm$  SD. Student's *t* test and ANOVA followed by the Bonferroni or Dunn's post hoc tests were used and considered significant at least a  $P < 0.05$ .

## **Results**

### *Oxidative stress enhances, but not initiates, endothelial cell migration*

To test whether oxidative stress enhances EC migration, we evaluated adherence and spreading properties in the presence or absence of the cellular oxidizing agent hydrogen peroxide ( $H_2O_2$ ). As shown in Fig. 1A,  $H_2O_2$  promoted an increase in cell adhesion. Additionally, cells were seeded onto collagen-coated plates in the presence or absence of  $H_2O_2$  to determine whether the oxidant affected EC spreading on a collagen matrix. Figs. 1B–D depict crystal violet-stained cells and demonstrate that  $H_2O_2$ -treated ECs have greater cell spreading extension over the matrix compared with vehicle-treated ECs. Quantification for this experiment showed a significant increase in the proportion of cells spread after  $H_2O_2$  exposure (Fig. 1E), which suggests that the oxidant induces enhanced cell migration.

Next, we used a transwell cell migration assay, wherein ECs were placed on a top chamber with a higher concentration of serum added to the lower chamber to create a serum gradient for chemotactic stimulation. The experiments were performed in the presence or absence of  $H_2O_2$ . Our results show an increase in  $H_2O_2$ -treated EC migration (Figs. 2A–C), and EC migration with the oxidant was greater than under vehicle-treatment conditions (Fig. 2D).

Furthermore, we used a cell monolayer-wounding assay to evaluate whether  $H_2O_2$  could induce EC migration. Significant increases in cell migration were measured through observing wound closure when ECs were exposed to 0.1 to 10  $\mu$ M of  $H_2O_2$  after 6 and 8 h compared with vehicle-treated cells (Figs. 3A–B). In addition, the migrated distance was severely augmented in ECs exposed to  $H_2O_2$  (Fig. 3C).

Changes in cell proliferation and viability interfere with cell migration analyses. We performed our experiments in a culture system using a low serum culture medium to avoid changes in proliferation or viability. We did not observe a significant increase in cell proliferation or viability under the conditions used herein (Supp. Fig. 1). It has been demonstrated that oxidative stress modulates cell proliferation and viability (Simon and Stutzin, 2008), which may interfere with cell migration analyses. We performed experiments at several  $H_2O_2$  concentrations to evaluate whether the  $H_2O_2$  challenge could modify cell proliferation and viability. We did not observe a significant change in cell proliferation or viability induced by  $H_2O_2$  (Supp. Fig. 2). Thus, under the experimental conditions used herein, neither cell proliferation nor viability interfered with our experiments.

Next, we were prompted to explore whether endogenous generation of ROS is able to increase EC migration. Considering that NAD(P)H oxidase (NOX) is a important source of intracellular ROS we used the NOX agonist, phorbol myristate acetate (PMA). PMA is a well-known stimuli often used to activate NOX (Bevilacqua et al., 2012; Gomes et al., 2012; Nomura et al., 2007; Price et al., 2002; Sumagin et al., 2013). ECs were cultured in the presence or absence PMA and cell migration experiments by means of monolayer-wounding assay were performed. Significant increase in cell migration was observed when ECs were exposed to different concentrations of PMA (Fig. 4A). In addition, the migrated distance was augmented in ECs exposed to PMA

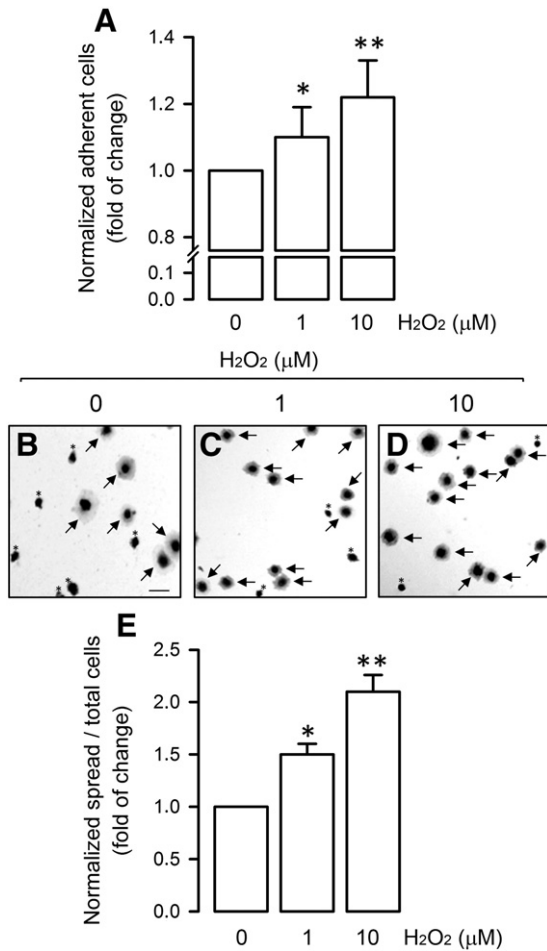


**Fig. 1.** H<sub>2</sub>O<sub>2</sub> exposure increases cell adhesion and spreading. (A) ECs were incubated in the absence or presence of H<sub>2</sub>O<sub>2</sub> (1, and 10 μM) for 20 min. Then, cells were removed and adherent cells were fixed and stained with crystal violet. Cells were solubilized, and the released crystal violet was measured. Determinations were done at least in triplicates and results are expressed as fold of change relative to vehicle-treated condition (0 μM H<sub>2</sub>O<sub>2</sub>). Statistical differences were assessed by one-way analysis of variance (ANOVA) (Kruskal–Wallis) followed by Dunn's post hoc test. \*:  $P < 0.05$ , \*\*:  $P < 0.01$  against vehicle-treated condition. Graph bars show the mean  $\pm$  SD (N = 4–5). (B–D) Representative images obtained from ECs in the absence (B) or presence of H<sub>2</sub>O<sub>2</sub> (1 (C), and 10 (D) μM) for 40 min and stained with crystal violet. Arrows indicate spread cells. Asterisks indicate non-spread cells. Bar scale represents 40 μm. (E) Bar graph summarizing several experiments as showed in (B–D). Results are expressed as the ratio of spread cells/total cells normalized as the fold of change relative to vehicle-treated condition (0 μM H<sub>2</sub>O<sub>2</sub>). Statistical differences were assessed by one-way analysis of variance (ANOVA) (Kruskal–Wallis) followed by Dunn's post hoc test. \*:  $P < 0.05$ , \*\*:  $P < 0.01$  against vehicle-treated condition. Graph bars show the mean  $\pm$  SD (N = 4–5).

(Fig. 4B). In agreement to this, similar results were obtained by means of Boyden chamber strategy (Supp. Fig. 3).

Our monolayer-wounding assay showed that ECs cultured in 1% FBS for 8 h had a low basal migration at ~15%, whereas in 0% FBS cultured for 8 h, cell migration changes were not observed (Supp. Fig. 4). We wondered whether H<sub>2</sub>O<sub>2</sub> can initiate endothelial cell migration in cultures without basal migration (in 0% FBS). Therefore, we performed experiments on ECs cultured in 1 and 0% serum in the presence or absence of H<sub>2</sub>O<sub>2</sub>. Hydrogen peroxide exposure did not evoke endothelial migration for cells cultured in 0% serum (Fig. 5A). Furthermore, the migrated distance did not change (Fig. 5B). These results suggest that H<sub>2</sub>O<sub>2</sub> can enhance endothelial migration, but it cannot initiate static EC migration.

Considering that cellular metabolism of living cells is characterized by a permanent generation of ROS, we evaluated whether reducing agents inhibit basal EC migration as a consequence of decreasing the intracellular oxidative status. The reducing agent dithiothreitol (DTT) was added to the culture medium, and a migration assay was performed.

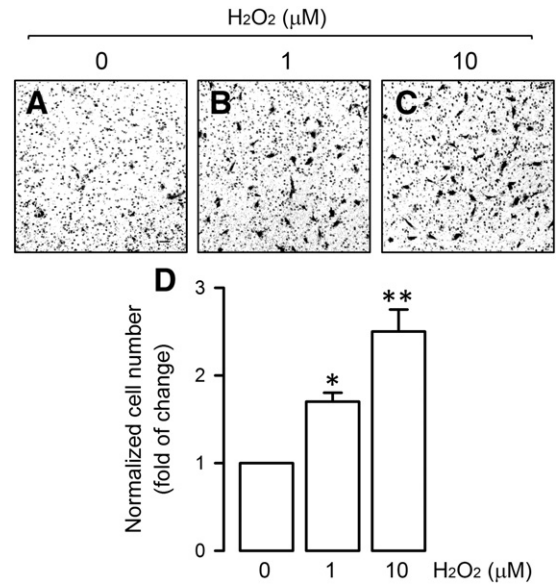


**Fig. 2.** H<sub>2</sub>O<sub>2</sub> exposure increases cell migration measured by Boyden-chamber migration assay. (A–C) Representative images obtained from ECs incubated in the absence (A) or presence of H<sub>2</sub>O<sub>2</sub> (1 (B), and 10 (C) μM) and subjected to Transwell migration assay. ECs were placed in the upper compartment of a Transwell chamber in 1% of FBS. In the lower chamber 10% FBS was added. Migration was allowed to occur for 24 h and migrated were fixed and stained with crystal violet. Bar scale represents 50 μm. (D) Bar graph summarizing several experiments as showed in (A–C). Results are expressed as fold of change relative to vehicle-treated condition (0 μM H<sub>2</sub>O<sub>2</sub>). Statistical differences were assessed by one-way analysis of variance (ANOVA) (Kruskal–Wallis) followed by Dunn's post hoc test. \*:  $P < 0.05$ , \*\*:  $P < 0.01$  against vehicle-treated condition. Graph bars show the mean  $\pm$  SD (N = 4–5).

DTT exposure significantly decreased EC migration (Fig. 6A). Further, the migrated distance was severely decreased with DTT (Fig. 6B). Concordant results were obtained by means of Boyden chamber strategy (Supp. Fig. 5A). We did not observe a significant change in cell viability using DTT (Supp. Fig. 6A). In the same line, we studied the effect of the ROS scavenger N-acetyl cysteine (NAC) in the basal migration of endothelial cells. Cells exposed to NAC showed decreased EC migration and migrated distance (Figs. 6C–D). Similar results were obtained by means of Boyden chamber strategy (Supp. Fig. 5B). We did not observe a significant change in cell viability using NAC (Supp. Fig. 6B). Next, we studied whether NOX activity was involved in the basal EC migration. To that end, we used the NOX inhibitors diphenyleneiodonium (DPI) and apocynin (Apo). DPI and Apo exposure significantly decreased EC migration (Figs. 6E and G, respectively). Further, the distance migrated was severely decreased with DPI and Apo (Figs. 6F and H, respectively). Comparable results were obtained by means of Boyden chamber strategy (Supp. Fig. 5C (for DPI) and 5D (for Apo)). We did not observe a significant change in cell viability neither using DPI nor Apo (Supp. Figs. 6C and D, respectively). These results suggest that the NAD(P)H oxidase are involved in the mechanism of EC migration.

#### Oxidative stress enhanced-endothelial cell migration depends on the TRPM4 ion channel

Considering that H<sub>2</sub>O<sub>2</sub> regulates TRPM4 expression (Simon et al., 2010), and TRPM4 is involved in immune cell migration (Barbet et al., 2008; Shimizu et al., 2009), we studied whether TRPM4 is involved in oxidative stress-enhanced EC migration. Although specific inhibitors are not available for TRPM4, the sulfonylurea glibenclamide inhibits the receptor-channel complex SUR1/TRPM4 with high affinity and specificity (Chen et al., 2003). Additionally, the hydroxytricyclic compound 9-phenanthrol rapidly inhibits the TRPM4 current without affecting its homolog, TRPM5 (Grand et al., 2008). 9-Phenanthrol inhibited H<sub>2</sub>O<sub>2</sub>-enhanced EC migration (Fig. 7A) and reduced the

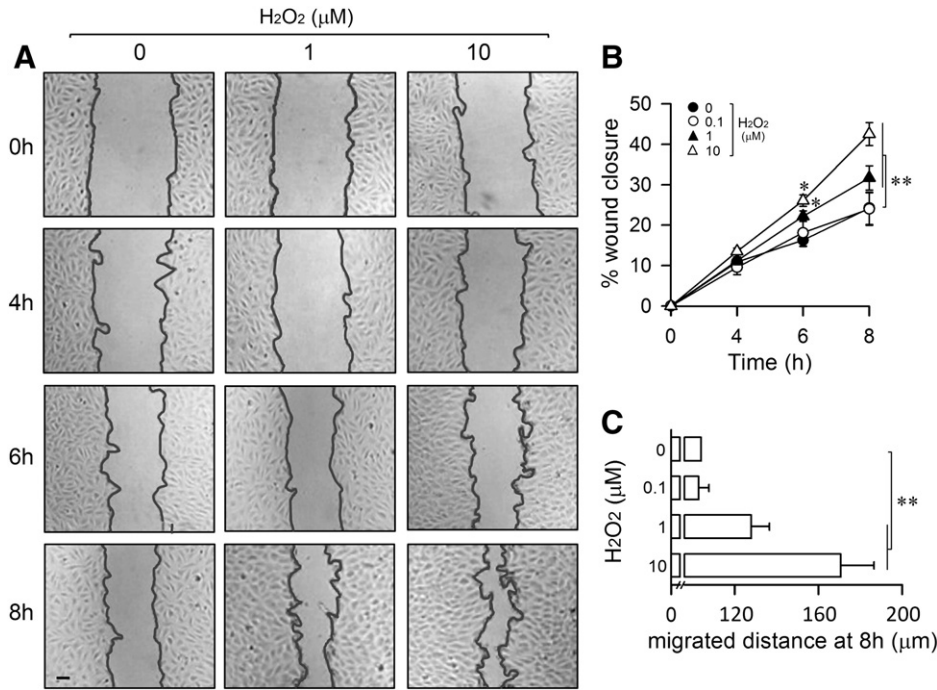


**Fig. 3.** H<sub>2</sub>O<sub>2</sub> exposure increases cell migration measured by wound-closure assay. (A) Representative images obtained from ECs incubated in the absence or presence of H<sub>2</sub>O<sub>2</sub> (1, and 10 μM) and subjected to a wound-closure assay. Images were taken at 0, 4, 6, and 8 h. To visualize the uncovered area of each wound, cell margins were outlined in each image. Bar scale represents 50 μm. Results are expressed in percentage relative to vehicle-treated condition (0 μM H<sub>2</sub>O<sub>2</sub>). (B) Graph summarizing several experiments as showed in (A), in which ECs were incubated in the absence or presence of H<sub>2</sub>O<sub>2</sub> (0.1, 1, and 10 μM). (C) Bar graph showing the migrated distance at 8 h from several experiments as showed in (A), in which ECs were incubated in the absence or presence of H<sub>2</sub>O<sub>2</sub> (0.1, 1, and 10 μM). Statistical differences were assessed by one-way analysis of variance (ANOVA) (Kruskal–Wallis) followed by Dunn's post hoc test. \*: *P* < 0.05, \*\*: *P* < 0.01 against vehicle-treated condition at 8 h. Graph bars show the mean ± SD (N = 5–6).

migrated distance (Fig. 7B), which suggests participation of TRPM4 ion channel. Similar results were observed with lower 9-phenanthrol doses (Supp. Figs. 7A and B). Similarly, Fig. 7C shows that glibenclamide reduced H<sub>2</sub>O<sub>2</sub>-enhanced EC migration. Consistently, glibenclamide treatment also reduced the H<sub>2</sub>O<sub>2</sub>-stimulated migrated distance (Fig. 7D). Similar results were generated using a lower glibenclamide dose (Supp. Figs. 7C and D).

Next, we studied whether H<sub>2</sub>O<sub>2</sub> induces the TRPM4 activity. Considering that TRPM4 activation generates plasma membrane depolarization (Becerra et al., 2011; Simon et al., 2010), we tested whether H<sub>2</sub>O<sub>2</sub> exposure induces cell depolarization as a measuring of TRPM4 activity. ECs exposed to H<sub>2</sub>O<sub>2</sub> showed a significant depolarization suggesting that H<sub>2</sub>O<sub>2</sub> induced the TRPM4 activity (Fig. 8A). These results are in agreement with data previously reported (Becerra et al., 2011; Simon et al., 2010).

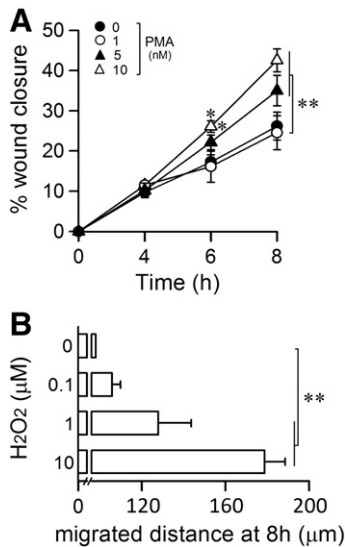


**Fig. 4.** PMA-induced endogenous generation of ROS increases cell migration. (A) ECs were subjected to wound-closure assay in the absence or presence of PMA (0, 1, 5, and 10 nM). Results are expressed in percentage relative to vehicle-treated condition (0 nM PMA). (B) Bar graph showing the migrated distance at 8 h from several experiments as showed in (A). Statistical differences were assessed by one-way analysis of variance (ANOVA) (Kruskal–Wallis) followed by Dunn's post hoc test. \*: *P* < 0.05, \*\*: *P* < 0.01 against vehicle-treated condition at 8 h. Graph bars show the mean ± SD (N = 5–6).

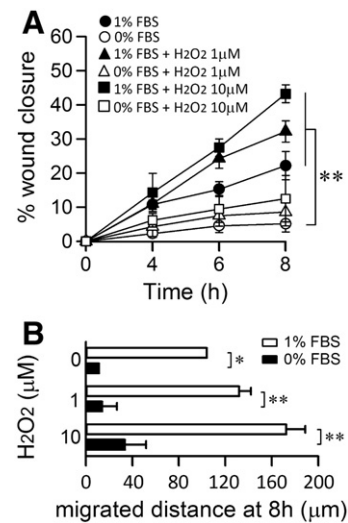


**Fig. 5.** H<sub>2</sub>O<sub>2</sub> enhances, but not initiates EC migration. (A) ECs were subjected to wound-closure assay in the absence or presence of H<sub>2</sub>O<sub>2</sub> (1 and 10 μM) and coincubated with 1% and 0% FBS. Results are expressed in percentage relative to vehicle-treated condition (0 μM H<sub>2</sub>O<sub>2</sub>). (B) Bar graph showing the migrated distance at 8 h from several experiments as showed in (A). Statistical differences were assessed by two-way analysis of variance (ANOVA) followed by Bonferroni post hoc test. \*: *P* < 0.05, \*\*: *P* < 0.01 against vehicle-treated condition at 8 h. Graph bars show the mean ± SD (N = 5–6).

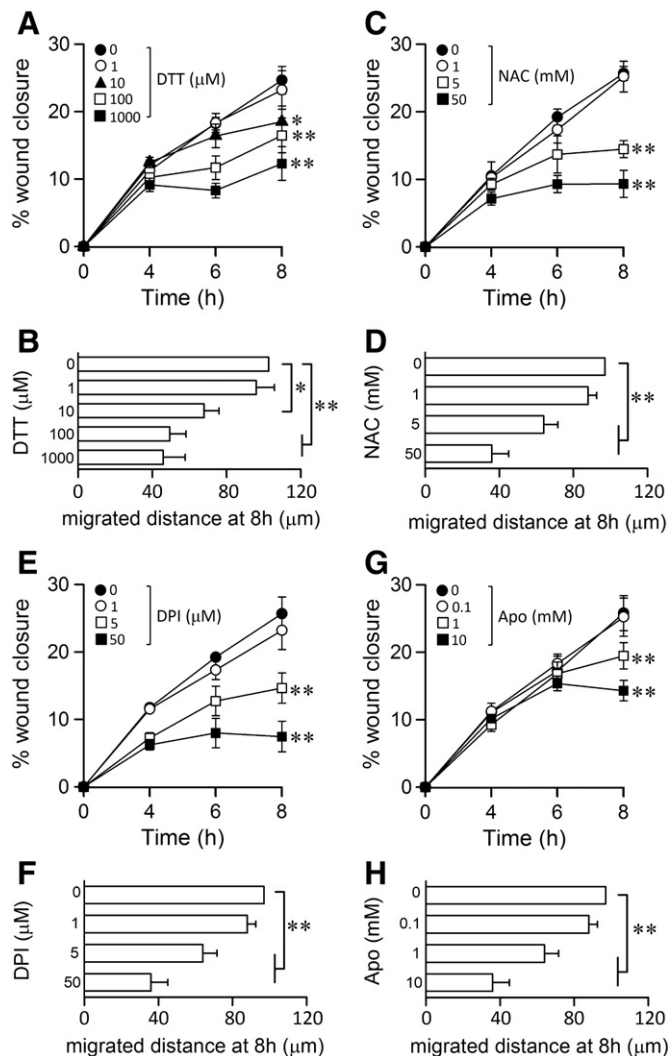


**Fig. 6.** The reducing agent DTT, the antioxidant compounds NAC, and the NAD(P)H oxidase inhibitors DPI and Apocynin, inhibit basal EC migration. (A–H) ECs were subjected to wound-closure assay in the absence or presence of DTT (1, 10, 100 and 1000  $\mu$ M) (A), NAC (1, 5, and 50 mM) (C), DPI (1, 5, and 50  $\mu$ M) (E), and Apo (0.1, 1, and 10  $\mu$ M) (G) at 1% FBS. Results are expressed in percentage relative to vehicle-treated condition. (B, D, F, and H). Bar graphs showing the migrated distance at 8 h from several experiments as shown in A, C, E, and G, respectively. Statistical differences were assessed by one-way analysis of variance (ANOVA) (Kruskal–Wallis) followed by Dunn's post hoc test. \*:  $P < 0.05$ , \*\*:  $P < 0.01$  against vehicle-treated condition at 8 h. Graph bars show the mean  $\pm$  SD ( $N = 3–6$ ).

To corroborate our pharmacological-based results, we used small interference RNA (siRNA) to knockdown TRPM4 expression and unequivocally demonstrate that TRPM4 participates in  $H_2O_2$ -enhanced EC migration. ECs were transfected with a specific siRNA against the human TRPM4 isoform (siRNA-TRPM4) or a non-targeting siRNA (siRNA-CTRL) used as a control. The transfected ECs were exposed to  $H_2O_2$  and subsequently analyzed by means of migration assays. The siRNA efficiency for TRPM4 expression downregulation was  $>95\%$  analyzed at mRNA (Fig. 8B) and protein level (Figs. 8C–D). To evaluate the loss of functionality of TRPM4 in ECs transfected with siRNA-TRPM4, ECs transfected with siRNA-TRPM4 or siRNA-CTRL were exposed to  $H_2O_2$  and cell depolarization was measured. ECs transfected with a siRNA-CTRL and exposed to  $H_2O_2$  showed a significant depolarization similar than that observed in non-transfected ECs exposed to  $H_2O_2$  showed in Fig. 8A (Fig. 8E), whereas ECs transfected with siRNA-TRPM4 and exposed to  $H_2O_2$  showed a decreased depolarization similar to that observed in non-transfected ECs in the absence of  $H_2O_2$  (Fig. 8E). These results suggest that siRNA-TRPM4 is efficient to downregulate the expression and function of TRPM4 ion channel.

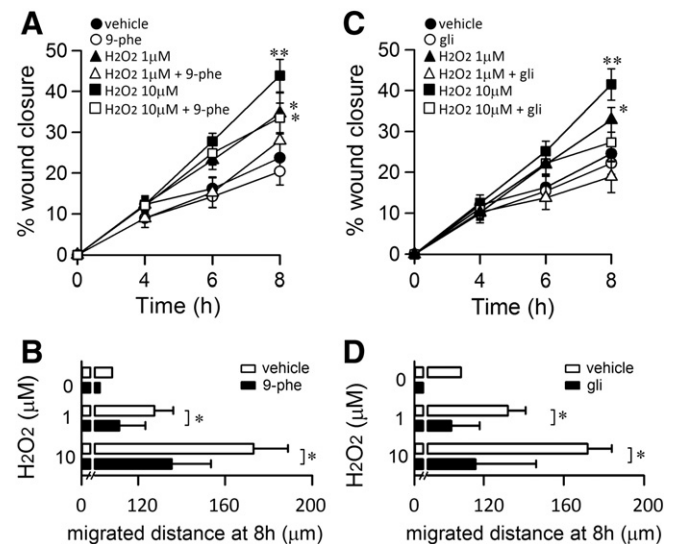


**Fig. 7.** TRPM4 inhibitors 9-phenanthrol, and glibenclamide diminish the  $H_2O_2$ -enhanced endothelial cell migration. ECs were subjected to wound-closure assay in the absence or presence of  $H_2O_2$  (1 and 10  $\mu$ M) and coincubated with 1  $\mu$ M 9-phenanthrol (9-phe) (A), and 100  $\mu$ M glibenclamide (gli) (C). Results are expressed in percentage relative to vehicle-treated condition (0  $\mu$ M  $H_2O_2$ ). (B–D) Bar graph showing the migrated distance at 8 h from several experiments as showed in (A–C, respectively). Statistical differences were assessed by two-way analysis of variance (ANOVA) followed by Bonferroni post hoc test. \*:  $P < 0.05$ , \*\*:  $P < 0.01$  against vehicle-treated condition at 8 h. Graph bars show the mean  $\pm$  SD ( $N = 5–6$ ).

ECs transfected with siRNA-CTRL showed increased cell adhesion after  $H_2O_2$  exposure (Fig. 8F), similar to observations in  $H_2O_2$ -treated non-transfected cells. In contrast,  $H_2O_2$ -treated ECs transfected with siRNA-TRPM4 showed a significantly inhibited  $H_2O_2$ -mediated EC adhesion (Fig. 8F).

Consistent with the cell-adhesion experiments,  $H_2O_2$ -treated ECs transfected with siRNA-CTRL showed an increase in cell spreading extension (Figs. 8G–I), which was similar to observations in  $H_2O_2$ -treated non-transfected cells, whereas  $H_2O_2$ -treated ECs transfected with siRNA-TRPM4 abolished  $H_2O_2$ -mediated cell spreading extension (Figs. 8J–L). The Fig. 8M shows the quantification for this experiment showing that TRPM4 downregulation inhibited  $H_2O_2$ -mediated cell spreading to vehicle-treatment levels.

Furthermore, we assayed migratory behavior using the Boyden-transwell migration assay. ECs transfected with siRNA-CTRL and exposed to  $H_2O_2$  showed increased cell migration (Figs. 9A–B and E) similar to the  $H_2O_2$ -treated non-transfected cells, whereas ECs transfected with siRNA-TRPM4 and exposed to  $H_2O_2$  showed significantly inhibited EC migration (Figs. 9C–D and E).

Moreover, ECs transfected with siRNA-CTRL and exposed to  $H_2O_2$  showed a greater wound closure percentage (Figs. 10A–B and E) similar to that observed in  $H_2O_2$ -treated non-transfected cells and an increased migrated distance (Fig. 10F). In contrast, ECs transfected with siRNA-TRPM4 showed inhibited  $H_2O_2$ -enhanced EC wound closure (Figs. 10C–D, E) and a decreased migrated distance (Fig. 10F).

## Discussion

During systemic inflammation, mediators of inflammation-derived ROS directly interact with ECs inside the blood vessel wall. As a result of the ROS challenge, ECs acquire several properties, including exacerbated migration features. Although certain data have been reported to describe the mechanism involved in oxidative stress-mediated EC migration, primarily to discern participation by intracellular redox-sensitive kinases and phosphatases, whether ROS-modulated ion channels in the plasma membrane are involved remains unknown.

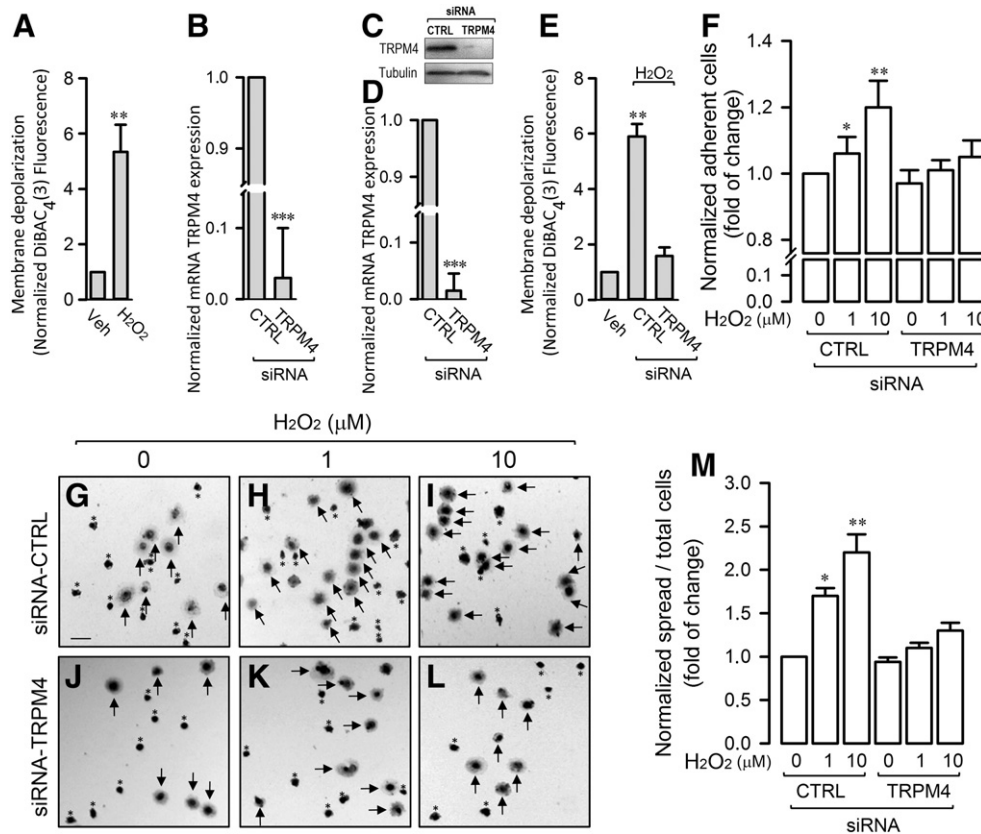


**Fig. 8.** TRPM4 downregulation inhibits H<sub>2</sub>O<sub>2</sub>-mediated cell adhesion and spreading. (A) Changes in membrane depolarization in ECs exposed in the absence or presence of H<sub>2</sub>O<sub>2</sub> as a measure of TRPM4 activity. Results are expressed relative to vehicle-treated condition as fold of change. Statistical differences were assessed by student's *t*-test (Mann–Whitney). \*\*, *P* < 0.01. Graph bars show the mean ± SD (*N* = 3). (B) Changes in the expression of mRNA of TRPM4 by qPCR. Endothelial cells were transfected with a specific siRNA against human isoform of TRPM4 (siRNA-TRPM4) and a non-targeting siRNA (siRNA-CTRL) used as a control. Results are expressed relative to cells transfected with siRNA-CTRL condition and normalized against 28S. Statistical differences were assessed by student's *t*-test (Mann–Whitney). \*\*\*, *P* < 0.001. Graph bars show the mean ± SD (*N* = 3). (C–D) Changes in the expression of the protein of TRPM4 by Western blot. Endothelial cells were transfected with siRNA-TRPM4 and siRNA-CTRL and then protein expression was analyzed. (C) Representative images from Western blot experiments performed for detection of TRPM4. (D) Densitometric analyses from several experiments, as shown in (C). Protein levels were normalized against tubulin, and the data are expressed relative to siRNA-CTRL. Statistical differences were assessed by student's *t*-test (Mann–Whitney). \*\*\*, *P* < 0.001. Graph bars show the mean ± SD (*N* = 3). (E) Changes in membrane depolarization induced by H<sub>2</sub>O<sub>2</sub> exposition in ECs transfected with siRNA-TRPM4 or siRNA-CTRL as a measure of the downregulation of the TRPM4 activity. Results are expressed relative to vehicle-treated condition as fold of change. Statistical differences were assessed by student's *t*-test (Mann–Whitney). \*\*, *P* < 0.01. Graph bars show the mean ± SD (*N* = 3). (F) ECs transfected with siRNA-TRPM4 and siRNA-CTRL, were incubated in the absence or presence of H<sub>2</sub>O<sub>2</sub> (1, and 10 μM) for 20 min. Then, cells were removed and adherent cells were fixed and stained with crystal violet. Cells were solubilized, and the released crystal violet was measured. Results are expressed as fold of change relative to non-transfected vehicle-treated condition (0 μM H<sub>2</sub>O<sub>2</sub>). Statistical differences were assessed by one-way analysis of variance (ANOVA) (Kruskal–Wallis) followed by Dunn's post hoc test. \*, *P* < 0.05; \*\*, *P* < 0.01 against non-transfected vehicle-treated condition. Graph bars show the mean ± SD (*N* = 5–6). (G–L) Representative images obtained from ECs transfected with a siRNA-CTRL (G–L) or siRNA-TRPM4 (J–L) in the absence (G and J) or presence of H<sub>2</sub>O<sub>2</sub> (1 (H and K), and 10 (I and L) μM) for 40 min and stained with crystal violet. Arrows indicate spread cell. Asterisks indicate non-spread cells. Bar scale represents 40 μm. (M) Bar graph summarizing several experiments as showed in (G–L). Results are expressed as the ratio of spread cells/total cells normalized as the fold of change relative to non-transfected vehicle-treated condition (0 μM H<sub>2</sub>O<sub>2</sub>). Statistical differences were assessed by one-way analysis of variance (ANOVA) (Kruskal–Wallis) followed by Dunn's post hoc test. \*, *P* < 0.05; \*\*, *P* < 0.01 against non-transfected vehicle-treated condition. Graph bars show the mean ± SD (*N* = 5–6).

In this study, we demonstrated that H<sub>2</sub>O<sub>2</sub> enhances EC migration in a dose-dependent manner but does not initiate movement in static cells without immune cell-derived chemoattractants. Furthermore, TRPM4 downregulation significantly decreased H<sub>2</sub>O<sub>2</sub>-enhanced EC migration, which suggests that TRPM4 is critical to H<sub>2</sub>O<sub>2</sub>-enhanced EC migration.

Cell migration is an important feature for several normal processes. However, increases in cell migration provoke abnormal responses and contribute to tumor angiogenesis, anomalous reendothelialization, and atherosclerosis (Pourgholami et al., 2008; Seetharam et al., 2006; Wang et al., 2011).

Increased cell adhesion and spreading indicate enhanced cell migration, and our results show that H<sub>2</sub>O<sub>2</sub> increases cell adhesion and spreading. These results are consistent with the experiments performed to determine cell migration, such as the transwell and wound-closure assays. Hence, diverse experimental strategies indicate that H<sub>2</sub>O<sub>2</sub> promotes a significant increase in EC migration.

An interesting finding is that H<sub>2</sub>O<sub>2</sub> cannot initiate migration in static ECs but only enhances basal migration. At low serum concentrations,

endothelial cells exhibit a minimal but significant basal migration, whereas under conditions of absolute absence of serum, the ECs were statistically static. Treatment with H<sub>2</sub>O<sub>2</sub> only induces enhanced cell migration, it does not initiate cell movement. We speculate that H<sub>2</sub>O<sub>2</sub> stimulates the synthesis of multiple intracellular factors, which are not sufficient to generate migration. Thus, several factors in the serum must be necessary to trigger migration.

The ROS participation in controlling EC migration has been broadly reported. Using the typical migratory stimuli for ECs (VEGF), several studies have reported that ROS generated from NOX activity and mitochondria is critical for EC migration (Ikeda et al., 2005; Kaplan et al., 2011; Pendyala et al., 2009; Ushio-Fukai, 2006; Wang et al., 2011; Yamaoka-Tojo et al., 2004). The ROS-mediated migration may be a consequence of oxidative molecules that modify activity in several protein kinases and phosphatases (Ikeda et al., 2005; Kaplan et al., 2011; Ushio-Fukai, 2006; Yamaoka-Tojo et al., 2004). Thus, through oxidation of specific amino acidic residues in those proteins, oxidative molecule generation controls the balance between phosphorylation and

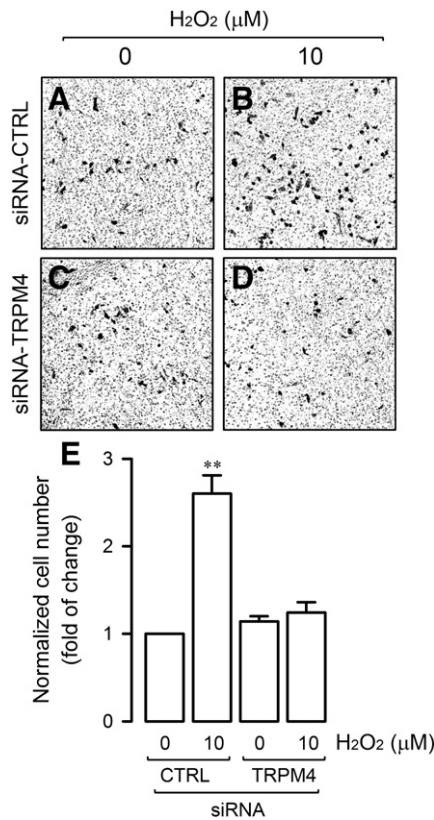


**Fig. 9.** TRPM4 downregulation inhibits H<sub>2</sub>O<sub>2</sub>-enhanced cell migration measured by Boyden-chamber migration assay. (A–D) Representative images obtained from ECs transfected with a non-targeting siRNA (siRNA-CTRL) (A–B) or siRNA against TRPM4 (siRNA-TRPM4) (C–D) were incubated in the absence (A and C) or presence of H<sub>2</sub>O<sub>2</sub> 10 μM (B and D) and subjected to Transwell migration assay. ECs were placed in the upper compartment of a Transwell chamber in 1% of FBS. In the lower chamber 10% FBS was added. Migration was allowed to occur for 24 h and migrated cells were fixed and stained with crystal violet. Bar scale represents 50 μm. (E) Bar graph summarizing several experiments as showed in (A–D). Results are expressed as fold of change relative to non-transfected vehicle-treated condition (0 μM H<sub>2</sub>O<sub>2</sub>). Statistical differences were assessed by one-way analysis of variance (ANOVA) (Kruskal–Wallis) followed by Dunn's post hoc test. \*:  $P < 0.05$ , \*\*:  $P < 0.01$  against non-transfected vehicle-treated condition. Graph bars show the mean  $\pm$  SD (N = 5–6).

dephosphorylation. Furthermore, ROS increases the expression and activation of the VEGFR2 and VEGFR3 to promote migration (Gonzalez-Pacheco et al., 2006; Wang et al., 2004a, 2004b). Besides, intracellular oxidative stress increases could trigger the activation of endogenous antioxidant pathways including, SOD, catalase, Nrf-2, and glutathione peroxidase (Droge, 2002). The activation of antioxidant mechanisms could also mediate the increase in migration stimulated by oxidative stress. In contrast, it has been reported that EC migration is inhibited by the CD-40 ligand through increased ROS generation (Urbich et al., 2002) and oxidized low-density lipoprotein (van Aalst et al., 2004). In our experiments, we used, at least, a 20-fold lower H<sub>2</sub>O<sub>2</sub> concentration compared with experiments that show H<sub>2</sub>O<sub>2</sub>-induced EC migration inhibition, which may explain the difference observed. Nevertheless, further experiments must be performed to better understand such inconsistencies.

In addition to ROS, nitric oxide (NO) is also an important regulator for EC migration. eNOS knockout mice show impaired angiogenesis in response to ischemia-induced oxidative stress (Murohara et al., 1999). Moreover, Akt/PKB-dependent VEGF-induced EC migration is increased through NO addition (Morales-Ruiz et al., 2000, 2001). These data suggest that several molecules, which produce an oxidative environment, contribute to increased EC migration.

The predominant vascular ROS source that promotes EC migration is a major concern. Intracellular ROS are generated by several endothelial

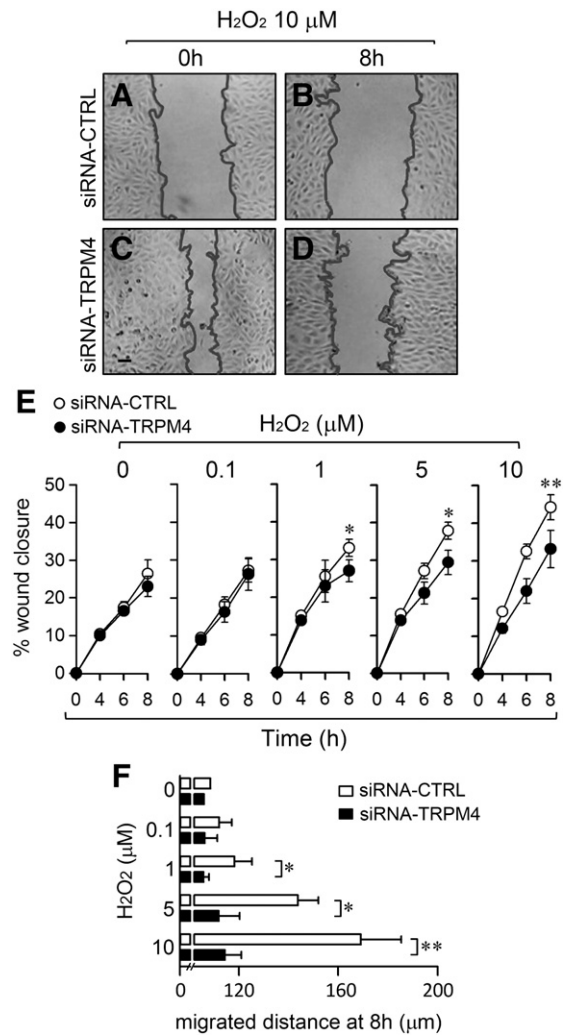


**Fig. 10.** TRPM4 downregulation inhibits H<sub>2</sub>O<sub>2</sub>-enhanced cell migration measured by wound-closure assay. (A–D) Representative images obtained from ECs transfected with a non-targeting siRNA (siRNA-CTRL) (A–B) or siRNA against TRPM4 (siRNA-TRPM4) (C–D) were incubated in the presence of 10 μM H<sub>2</sub>O<sub>2</sub> and subjected to a wound-closure assay. Images were taken at 0 and 8 h. To visualize the uncovered area of each wound, cell margins were outlined in each image. Bar scale represents 50 μm. (E) Graph summarizing several experiments as showed in (A–D), in which ECs transfected with siRNA-CTRL or siRNA-TRPM4 were incubated in the absence (A and C) or presence (B and D) of H<sub>2</sub>O<sub>2</sub> (0.1, 1, 5, and 10 μM). Results are expressed in percentage normalized relative to non-transfected vehicle-treated condition (0 μM H<sub>2</sub>O<sub>2</sub>). (F) Bar graph showing the migrated distance at 8 h from several experiments as showed in (A–D), in which ECs transfected with a non-targeting siRNA (siRNA-CTRL) (empty bar) or siRNA against TRPM4 (siRNA-TRPM4) (filled bar), were incubated in the absence or presence of H<sub>2</sub>O<sub>2</sub> (0.1, 1, 5, and 10 μM). Statistical differences were assessed by two-way analysis of variance (ANOVA) followed by Bonferroni post hoc test. \*:  $P < 0.05$ , \*\*:  $P < 0.01$  against vehicle-treated condition. Graph bars show the mean  $\pm$  SD (N = 4–6).

sources, including NOX, xanthine oxidase, the mitochondrial electron transport chain, and NO synthase (Cave et al., 2006; Griendling et al., 2000; Shin et al., 2008; Sorescu and Griendling, 2002; Takimoto et al., 2005). It has been reported that NOX-derived ROS stimulates EC migration (Ikeda et al., 2005; Kaplan et al., 2011; Ushio-Fukai, 2006; Yamaoka-Tojo et al., 2004). In addition, we previously demonstrated that NOX-2 and NOX-4 are important ROS sources in an endothelial model for endotoxin-induced systemic inflammation, which suggests that NOX may be important for EC migration (Simon and Fernandez, 2009). On the other hand, it has been reported that mitochondria-derived ROS promote EC migration, which suggests that mitochondria may be the relevant oxidant source (Wang et al., 2011). Further studies are necessary to better understand this mechanism.

Because changes in intracellular  $\text{Ca}^{2+}$  levels modulate cell migration, identifying a key calcium regulator that controls cell migration is an issue of major importance. In this context, the TRPM4 function as regulator for internal calcium levels suggests that this ion channel may be a plausible candidate. Herein, we demonstrate that TRPM4 is critical to oxidative stress-enhanced EC migration. These results are consistent with previous reports that TRPM4 activity controls mast and dendritic cell migration, through regulating intracellular calcium homeostasis (Barbet et al., 2008; Shimizu et al., 2009). Absence of TRPM4 expression in a mouse model of dendritic cells considerably impaired the chemokine-dependent dendritic cell migration (Barbet et al., 2008). Furthermore, mast cells TRPM4 deficient (TRPM4<sup>-/-</sup>), showed a lower migration compared to wild type cells (Shimizu et al., 2009).

Considering that inflammatory process are characterized by an increased intracellular ROS concentration, and ROS augment TRPM4 activity through abolishing the channel desensitization, we suggest that inflammation-induced ROS generation modulates TRPM4 activity to control EC migration. TRPM4 activity controls the plasma membrane potential and can prevent intracellular calcium overload through transient depolarization of the plasma membrane (Launay et al., 2002). Further, TRPM4 regulates the intracellular  $\text{Ca}^{2+}$  oscillations that control protein expression (Launay et al., 2004). Thus, TRPM4 activity changes directly affect intracellular calcium homeostasis, which may subsequently alter cell migration. Furthermore, suppression of the expression of TRPM4 modifies the cytokine production including IL-2, IL-4 and IFN-gamma in lymphocytes, which could alter cell migration (Launay et al., 2004; Weber et al., 2010). Additional studies are needed to demonstrate that similar alteration occurs in EC affecting endothelial migration.

The TRPM4 ion channel is highly expressed in the endothelia for different vessels, including arterial and vein endothelial cells. This study was performed using ECs from veins. Although it is reasonable to propose that TRPM4 modulates EC migration in all blood vessels, further experiments are necessary to support this hypothesis.

TRPM4 is an ion channel involved in tumor cells progression and metastasis. Those cells acquire a migratory phenotype to promote angiogenesis and migration to other tissues supports our findings. Because the tumor environment is predominantly oxidative, ROS-induced changes in TRPM4 activity correlate well with enhanced cancer cell migration.

Taken together, the findings reported here show that oxidative stress is effective at enhancing but not initiating cell migration. Thus, enhanced oxidative molecules alter normal motility for healthy ECs to increased pathogenic migration. Noteworthy, our findings demonstrate that TRPM4 is critical to oxidative stress-enhanced endothelial cell migration. These findings may be useful in understanding the molecular mechanism that controls EC migration during inflammation and as a potential pharmacological target for drug design to modulate EC migration under pathological conditions.

## Conflict of interest

The authors confirm that there are no conflicts of interest.

## Acknowledgments

This work was supported by research grants from the Fondo Nacional de Desarrollo Científico y Tecnológico – FONDECYT 1121078 (FS), 11121239 (OC), 1100995 (AE), 1130996 (CR), 1120380 (CCV), 1120240 (DV), and 1120712 (LAV). Millennium Institute on Immunology and Immunotherapy P09-016-F (FS, AE, CR), Centro para el Desarrollo de la Nanociencia y Nanotecnología (CEDENNA); FB0807 (LAV). Association-Francaise Contre Les Myopathies AFM 16670 (CCV), UNAB-DI-281-13/R (CCV) and UNAB DI-209-12/N (FS, AE, CR).

## Appendix A. Supplementary data

Supplementary data to this article can be found online at <http://dx.doi.org/10.1016/j.mvr.2014.02.001>.

## References

- Barbet, G., et al., 2008. The calcium-activated nonselective cation channel TRPM4 is essential for the migration but not the maturation of dendritic cells. *Nat. Immunol.* 9, 1148–1156.
- Becerra, A., et al., 2011. Transient receptor potential melastatin 4 inhibition prevents lipopolysaccharide-induced endothelial cell death. *Cardiovasc. Res.* 91, 677–684.
- Bevilacqua, E., et al., 2012. NADPH oxidase as an important source of reactive oxygen species at the mouse maternal-fetal interface: putative biological roles. *Reprod. Biomed. Online* 25, 31–43.
- Bryan, N., et al., 2012. Reactive oxygen species (ROS) – a family of fate deciding molecules pivotal in constructive inflammation and wound healing. *Eur. Cells Mater.* 24, 249–265.
- Cabello-Verrugio, C., et al., 2011. Fibrotic response induced by angiotensin-II requires NAD(P)H oxidase-induced reactive oxygen species (ROS) in skeletal muscle cells. *Biochem. Biophys. Res. Commun.* 410, 665–670.
- Cai, H., Harrison, D.G., 2000. Endothelial dysfunction in cardiovascular diseases: the role of oxidant stress. *Circ. Res.* 87, 840–844.
- Cave, A.C., et al., 2006. NADPH oxidases in cardiovascular health and disease. *Antioxid. Redox Signal.* 8, 691–728.
- Chen, M., et al., 2003. Functional coupling between sulfonylurea receptor type 1 and a nonselective cation channel in reactive astrocytes from adult rat brain. *J. Neurosci.* 23, 8568–8577.
- Closa, D., Folch-Puy, E., 2004. Oxygen free radicals and the systemic inflammatory response. *IUBMB Life* 56, 185–191.
- Cook-Mills, J.M., 2002. VCAM-1 signals during lymphocyte migration: role of reactive oxygen species. *Mol. Immunol.* 39, 499–508.
- Coso, S., et al., 2012. NADPH oxidases as regulators of tumor angiogenesis: current and emerging concepts. *Antioxid. Redox Signal.* 16, 1229–1247.
- Droge, W., 2002. Free radicals in the physiological control of cell function. *Physiol. Rev.* 82, 47–95.
- Echeverria, C., et al., 2013. Lipopolysaccharide induces a fibrotic-like phenotype in endothelial cells. *J. Cell. Mol. Med.* 17, 800–814.
- Fantozzi, I., et al., 2003. Hypoxia increases AP-1 binding activity by enhancing capacitative  $\text{Ca}^{2+}$  entry in human pulmonary artery endothelial cells. *Am. J. Physiol. Lung Cell. Mol. Physiol.* 285, L1233–L1245.
- Gomes, S.Z., et al., 2012. Expression of NADPH oxidase by trophoblast cells: potential implications for the postimplanting mouse embryo. *Biol. Reprod.* 86, 56.
- Gonzalez-Pacheco, F.R., et al., 2006. Mechanisms of endothelial response to oxidative aggression: protective role of autologous VEGF and induction of VEGFR2 by H2O2. *Am. J. Physiol. Heart Circ. Physiol.* 291, H1395–H1401.
- Goumans, M.J., et al., 2008. Transforming growth factor beta-induced endothelial-to-mesenchymal transition: a switch to cardiac fibrosis? *Trends Cardiovasc. Med.* 18, 293–298.
- Grand, T., et al., 2008. 9-phenanthrol inhibits human TRPM4 but not TRPM5 cationic channels. *Br. J. Pharmacol.* 153, 1697–1705.
- Griendling, K.K., et al., 2000. Modulation of protein kinase activity and gene expression by reactive oxygen species and their role in vascular physiology and pathophysiology. *Arterioscler. Thromb. Vasc. Biol.* 20, 2175–2183.
- Ikeda, S., et al., 2005. IQGAP1 regulates reactive oxygen species-dependent endothelial cell migration through interacting with Nox2. *Arterioscler. Thromb. Vasc. Biol.* 25, 2295–2300.
- Kaplan, N., et al., 2011. Localized cysteine sulfenic acid formation by vascular endothelial growth factor: role in endothelial cell migration and angiogenesis. *Free Radic. Res.* 45, 1124–1135.
- Kimura, C., et al., 2001. Alterations of  $\text{Ca}^{2+}$  mobilizing properties in migrating endothelial cells. *Am. J. Physiol. Heart Circ. Physiol.* 281, H745–H754.
- Launay, P., et al., 2002. TRPM4 is a  $\text{Ca}^{2+}$ -activated nonselective cation channel mediating cell membrane depolarization. *Cell* 109, 397–407.
- Launay, P., et al., 2004. TRPM4 regulates calcium oscillations after T cell activation. *Science* 306, 1374–1377.
- Lin, C.C., et al., 2012. NADPH oxidase 2-derived reactive oxygen species signal contributes to bradykinin-induced matrix metalloproteinase-9 expression and cell migration in brain astrocytes. *Cell Commun. Signal.* 10, 35.
- Lo, I.C., et al., 2005. Reactive oxygen species and ERK 1/2 mediate monocyte chemotactic protein-1-stimulated smooth muscle cell migration. *J. Biomed. Sci.* 12, 377–388.
- Lu, L., et al., 2013. Two-dimensional fluorescence in-gel electrophoresis of coronary restenosis tissues in minipigs: increased adipocyte fatty acid binding protein induces reactive oxygen species-mediated growth and migration in smooth muscle cells. *Arterioscler. Thromb. Vasc. Biol.* 33, 572–580.
- Luanpitpong, S., et al., 2010. Regulation of lung cancer cell migration and invasion by reactive oxygen species and caveolin-1. *J. Biol. Chem.* 285, 38832–38840.
- Morales, M.G., et al., 2012. Angiotensin II-induced pro-fibrotic effects require p38MAPK activity and transforming growth factor beta 1 expression in skeletal muscle cells. *Int. J. Biochem. Cell Biol.* 44, 1993–2002.
- Morales-Ruiz, M., et al., 2000. Vascular endothelial growth factor-stimulated actin reorganization and migration of endothelial cells is regulated via the serine/threonine kinase Akt. *Circ. Res.* 86, 892–896.

- Morales-Ruiz, M., et al., 2001. Sphingosine 1-phosphate activates Akt, nitric oxide production, and chemotaxis through a Gi protein/phosphoinositide 3-kinase pathway in endothelial cells. *J. Biol. Chem.* 276, 19672–19677.
- Muller, M.M., Griesmacher, A., 2000. Markers of endothelial dysfunction. *Clin. Chem. Lab. Med.* 38, 77–85.
- Murohara, T., et al., 1999. Role of endothelial nitric oxide synthase in endothelial cell migration. *Arterioscler. Thromb. Vasc. Biol.* 19, 1156–1161.
- Nagata, M., 2005. Inflammatory cells and oxygen radicals. *Curr. Drug Targets Inflamm. Allergy* 4, 503–504.
- Nilius, B., et al., 2003. Voltage dependence of the Ca<sup>2+</sup>-activated cation channel TRPM4. *J. Biol. Chem.* 278, 30813–30820.
- Nomura, N., et al., 2007. Phorbol 12-myristate 13-acetate (PMA)-induced migration of glioblastoma cells is mediated via p38MAPK/Hsp27 pathway. *Biochem. Pharmacol.* 74, 690–701.
- Nunez-Villena, F., et al., 2011. Increased expression of the transient receptor potential melastatin 7 channel is critically involved in lipopolysaccharide-induced reactive oxygen species-mediated neuronal death. *Antioxid. Redox Signal.* 15, 2425–2438.
- Pendyala, S., et al., 2009. Role of Nox4 and Nox2 in hyperoxia-induced reactive oxygen species generation and migration of human lung endothelial cells. *Antioxid. Redox Signal.* 11, 747–764.
- Potentia, S., et al., 2008. The role of endothelial-to-mesenchymal transition in cancer progression. *Br. J. Cancer* 99, 1375–1379.
- Pourgholami, et al., 2008. Inhibitors of vascular endothelial growth factor in cancer. *Cardiovasc. Hematol. Agents Med. Chem.* 6, 343–347.
- Price, M.O., Atkinson, S.J., Knaus, U.G., Dinauer, M.C., 2002. Rac activation induces NADPH oxidase activity in transgenic COSphox cells, and the level of superoxide production is exchange factor-dependent. *J. Biol. Chem.* 277, 19220–19228.
- Seetharam, D., et al., 2006. High-density lipoprotein promotes endothelial cell migration and reendothelialization via scavenger receptor-B type I. *Circ. Res.* 98, 63–72.
- Shimizu, T., et al., 2009. TRPM4 regulates migration of mast cells in mice. *Cell Calcium* 45, 226–232.
- Shin, M.H., et al., 2008. Reactive oxygen species produced by NADPH oxidase, xanthine oxidase, and mitochondrial electron transport system mediate heat shock-induced MMP-1 and MMP-9 expression. *Free Radic. Biol. Med.* 44, 635–645.
- Simon, F., Fernandez, R., 2009. Early lipopolysaccharide-induced reactive oxygen species production evokes necrotic cell death in human umbilical vein endothelial cells. *J. Hypertens.* 27, 1202–1216.
- Simon, F., Stutzin, A., 2008. Protein kinase C-mediated phosphorylation of p47 phox modulates platelet-derived growth factor-induced H<sub>2</sub>O<sub>2</sub> generation and cell proliferation in human umbilical vein endothelial cells. *Endothelium* 15, 175–188.
- Simon, F., et al., 2010. Hydrogen peroxide removes TRPM4 current desensitization conferring increased vulnerability to necrotic cell death. *J. Biol. Chem.* 285, 37150–37158.
- Simon, F., et al., 2013. Oxidative stress-modulated TRPM ion channels in cell dysfunction and pathological conditions in humans. *Cell. Signal.* 25, 1614–1624.
- Sorescu, D., Griendling, K.K., 2002. Reactive oxygen species, mitochondria, and NAD(P)H oxidases in the development and progression of heart failure. *Congest. Heart Fail.* 8, 132–140.
- Stone, J.R., Collins, T., 2002. The role of hydrogen peroxide in endothelial proliferative responses. *Endothelium* 9, 231–238.
- Sumagin, R., et al., 2013. Activation of PKCβ<sub>II</sub> by PMA facilitates enhanced epithelial wound repair through increased cell spreading and migration. *PLoS One* 8, e55775.
- Takimoto, E., et al., 2005. Oxidant stress from nitric oxide synthase-3 uncoupling stimulates cardiac pathologic remodeling from chronic pressure load. *J. Clin. Invest.* 115, 1221–1231.
- Tran, P.O., et al., 1999. A wound-induced [Ca<sup>2+</sup>]<sub>i</sub> increase and its transcriptional activation of immediate early genes is important in the regulation of motility. *Exp. Cell Res.* 246, 319–326.
- Urbich, C., et al., 2002. CD40 ligand inhibits endothelial cell migration by increasing production of endothelial reactive oxygen species. *Circulation* 106, 981–986.
- Ushio-Fukai, M., 2006. Redox signaling in angiogenesis: role of NADPH oxidase. *Cardiovasc. Res.* 71, 226–235.
- van Aalst, J.A., et al., 2004. Role of reactive oxygen species in inhibition of endothelial cell migration by oxidized low-density lipoprotein. *J. Vasc. Surg.* 40, 1208–1215.
- Van der Goes, A., et al., 2001. Reactive oxygen species enhance the migration of monocytes across the blood–brain barrier in vitro. *FASEB J.* 15, 1852–1854.
- Wang, J.F., et al., 2004a. Activation of vascular endothelial growth factor receptor-3 and its downstream signaling promote cell survival under oxidative stress. *J. Biol. Chem.* 279, 27088–27097.
- Wang, Z., et al., 2004b. Reactive oxygen species-sensitive p38 MAPK controls thrombin-induced migration of vascular smooth muscle cells. *J. Mol. Cell. Cardiol.* 36, 49–56.
- Wang, Y., et al., 2011. Regulation of VEGF-induced endothelial cell migration by mitochondrial reactive oxygen species. *Am. J. Physiol. Cell Physiol.* 301, C695–C704.
- Weber, K.S., et al., 2010. Trpm4 differentially regulates Th1 and Th2 function by altering calcium signaling and NFAT localization. *J. Immunol.* 185, 2836–2846.
- Wu, Y., et al., 1997. Inhibition of head and neck squamous cell carcinoma growth and invasion by the calcium influx inhibitor carboxyamido-triazole. *Clin. Cancer Res.* 3, 1915–1921.
- Yamaoka-Tojo, M., et al., 2004. IQGAP1, a novel vascular endothelial growth factor receptor binding protein, is involved in reactive oxygen species-dependent endothelial migration and proliferation. *Circ. Res.* 95, 276–283.
- Yoshikawa, N., et al., 1999. Gradients in cytoplasmic calcium concentration ([Ca<sup>2+</sup>]<sub>i</sub>) in migrating human umbilical vein endothelial cells (HUVECs) stimulated by shear stress. *Life Sci.* 65, 2643–2651.